A CLN6-CLN8 complex recruits lysosomal enzymes at the ER for Golgi transfer

Lakshya Bajaj, Jaiprakash Sharma, Alberto di Ronza, Pengcheng Zhang, Aiden Eblimit, Rituraj Pal, Dany Roman, John R. Collette, Clarissa Booth, Kevin T. Chang, Richard N. Sifers, Sung Y. Jung, Jill M. Weimer, Rui Chen, Randy W. Schekman and Marco Sardiello

Supplemental Material:

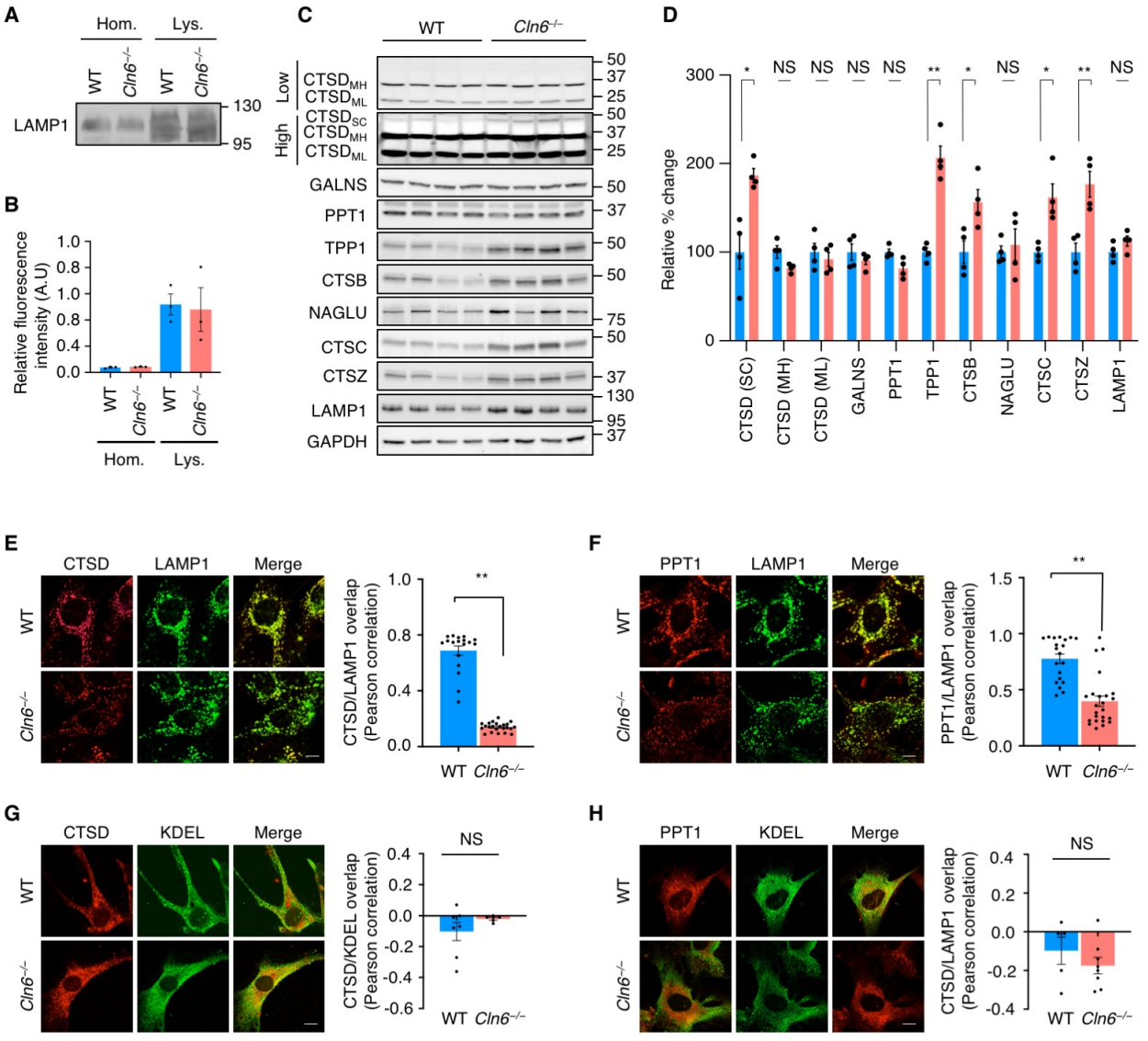

Supplemental Figure 1. Depletion of lysosomal enzymes upon CLN6 deficiency. (A) LAMP1 immunoblot showing lysosomal enrichment in collected fractions from WT and *Cln6*$^{-/-}$ samples. **(B)** HEX enzyme activity assay showing significant enrichment in the collected fractions from WT and *Cln6*$^{-/-}$ mice. Data are means ± SEM (n = 3). **(C)** Immunoblot analysis of liver homogenates from *Cln6*$^{-/-}$ mice and WT controls. **(D)** Band intensities were quantified and normalized to GAPDH. Data are means ± SEM (n = 4). (**E-H**) Confocal microscopy analysis of WT and *Cln6*$^{-/-}$ MEFs showing decreased overlap of the signals of endogenous CTSD and PPT1 with the lysosomal marker LAMP1 in *Cln6*$^{-/-}$ cells (**E** and **F**) and no changes in the overlap of CTSD and PPT1 with the ER marker KDEL (**G** and **H**). Data are means ± SEM; **E**, n = 18 (WT), n = 23 (*Cln6*$^{-/-}$); **F**, n = 20 (WT), n = 24 (*Cln6*$^{-/-}$); **G**, n = 5 (WT), n = 7 (*Cln6*$^{-/-}$); **H**, n = 5 (WT), n = 8 (*Cln6*$^{-/-}$). Statistical differences between groups were calculated using Student's t test; *$P < 0.05$, **$P < 0.01$; NS, not significant.

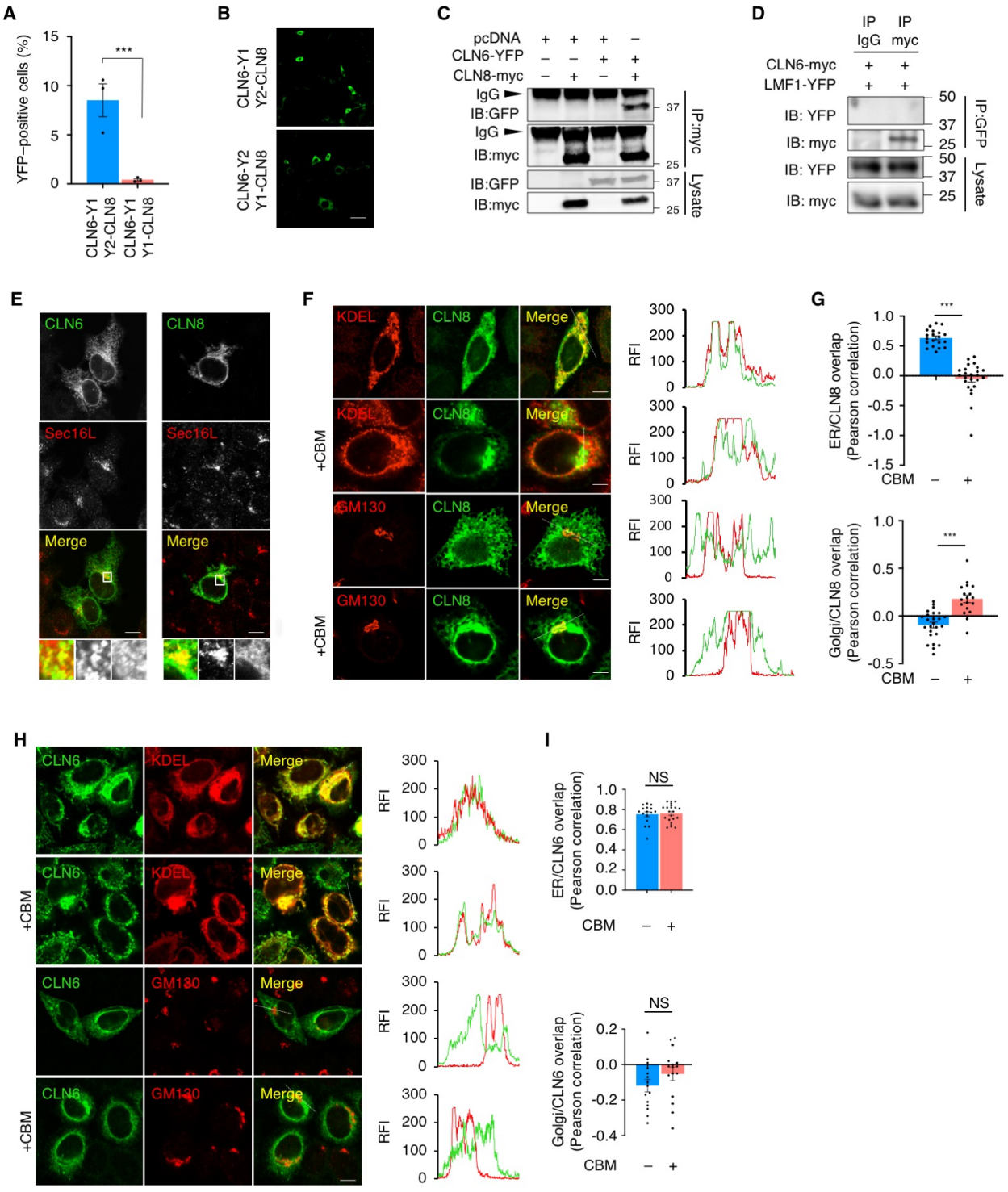

Supplemental Figure 2. Interaction and localization assays for CLN6. (A) BiFC assay of CLN6-Y1 with Y2-CLN8 in HeLa cells followed by flow cytometry. Data are means ± SEM (n = 3). (**B**) BiFC assay of CLN6-Y2 with Y1-CLN8 and CLN6-Y1 with Y2-CLN8 in MEFs followed by confocal microscopy. Green signals represent the reconstituted YFP. Scale bar: 200 µm. (**C-D**) Co-IP analysis of CLN6 with CLN8 (**C**) and LMF1 (**D**). All proteins were tagged as indicated and transiently expressed. Co-IP assays were performed using the indicated antibodies and IgG as a negative control. Lysate represents 10% of the total cell extract used for IP. **(E)** Confocal microscopy

showing that CLN6 and CLN8 colocalize with the ER exit site marker Sec16L (red). Scale bar: 20 μm. Inset magnifications (5x) are reported. (**F**) Confocal microscopy showing the subcellular localization of CLN8 upon treatment with CBM. Trace outline is used for line-scan analysis of Relative Fluorescence Intensity (RFI) of CLN8, GM130 (Golgi marker) and KDEL (ER marker) signals. Scale bar: 10 μm. (**G**) Pearson correlation analysis of the co-localization extent of full-length CLN8 and the ER marker KDEL or the Golgi marker GM130, with and without treatment with CBM. Data are means ± SEM; ER/CLN8 overlap, $n = 20$ (no CBM), $n = 24$ (CBM); Golgi/CLN8 overlap, $n = 18$ (no CBM), $n = 25$ (CBM). (**H**) Confocal microscopy showing that CLN6 resides in the ER upon treatment with CBM. Trace outline is used for RFI line-scan analysis of CLN6, GM130, and KDEL signals. Scale bar: 20 μm. (**I**) Pearson correlation analysis of the co-localization extent of CLN6 with KDEL or GM130 upon treatment with CBM. Data are means ± SEM; ER/CLN8 overlap, $n = 16$ (no CBM), $n = 22$ (CBM); Golgi/CLN8 overlap, $n = 15$ (no CBM), $n = 15$ (CBM). Statistical differences between groups were calculated using Student's *t* test (**A**, **G** and **I**); , $^{**}P < 0.01$, $^{***}P < 0.001$; NS, not statistically significant.

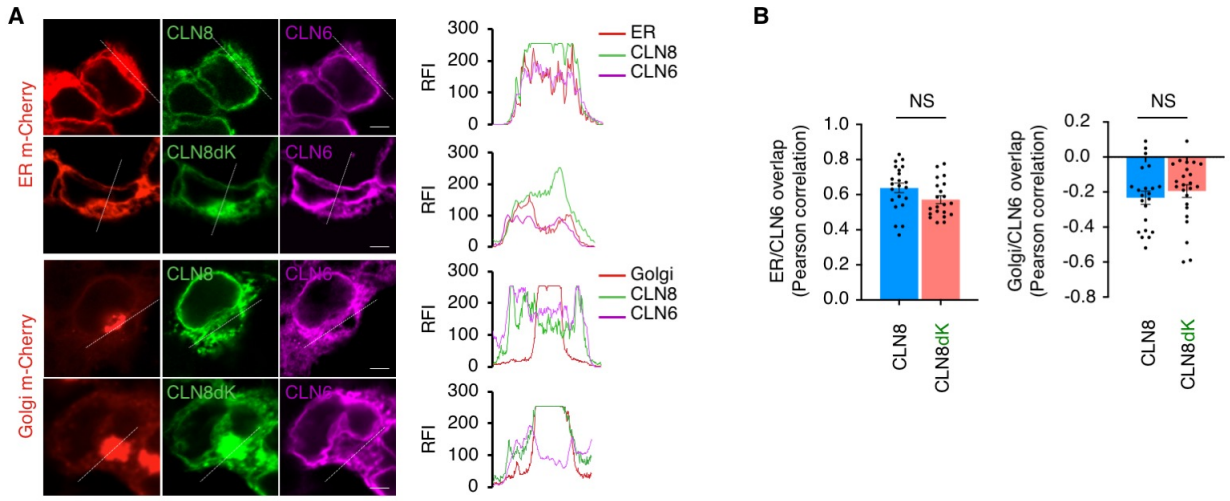

Supplemental Figure 3. CLN6 does not traffic to the Golgi in the presence of a Golgi-restricted CLN8 mutant. **(A)** Confocal microscopy analysis showing ER localization of full-length CLN6 and Golgi localization of CLN8-RRXX (CLN8-dK) upon cotransfection of the two constructs in *CLN6*$^{-/-}$ cells. Trace outline is used for line-scan analysis of Relative Fluorescence Intensity (RFI) of CLN8, CLN6, Golgi m-Cherry and ER m-Cherry signals. Scale bar: 10 µm. (**B**) Pearson correlation analysis of the co-localization extent of CLN6 with ER and Golgi markers when cotransfected with CLN8-dK in *CLN6*$^{-/-}$ cells. Data are means ± SEM; ER/CLN6 overlap, $n = 20$ (CLN8), $n = 24$ (CLN8dK); Golgi/CLN6 overlap, $n = 25$ (CLN8), $n = 18$ (CLN8dK). Statistical differences between groups were calculated using Student's *t* test; NS, not statistically significant.

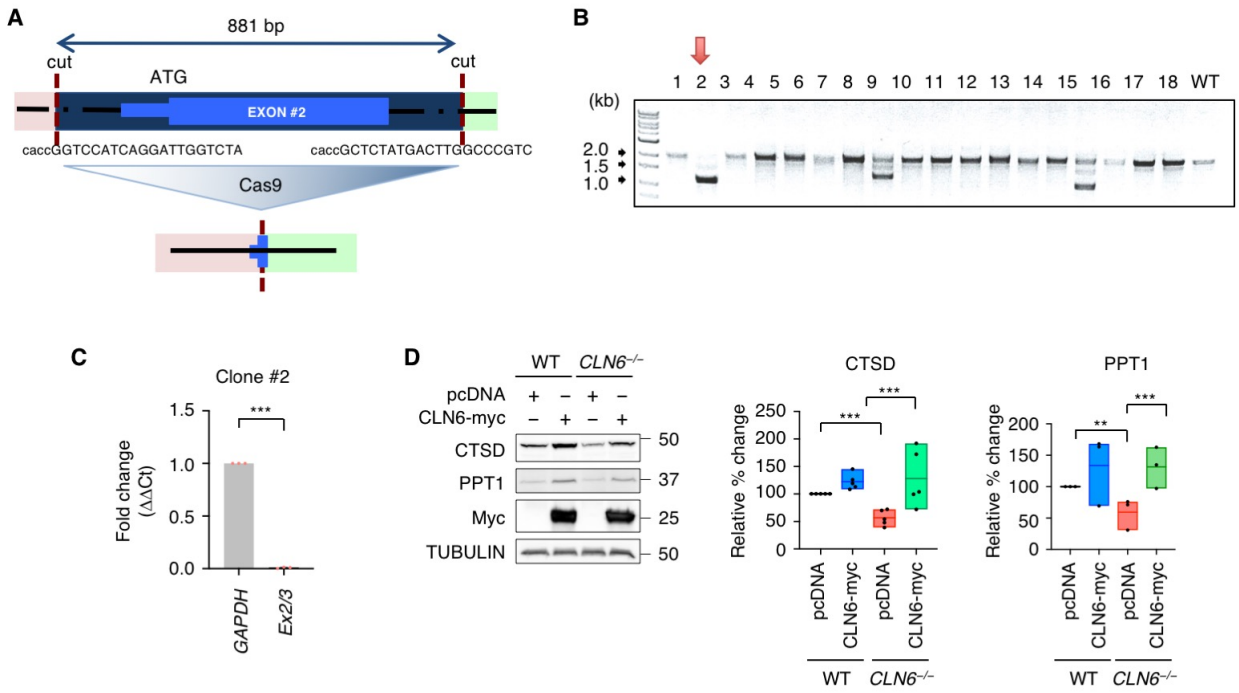

Supplemental Figure 4. Generation and validation of *CLN6*$^{-/-}$ cells. (A) Cartoon depicting the region from *CLN6* gene that was deleted to generate *CLN6*$^{-/-}$ cells by CRISPR/Cas9 genome editing. **(B)** PCR clone screening of individual HEK293-T cell lines to identify clones carrying deletion of *CLN6* exon 2 (CLN6$^{-/-}$) upon CRISPR/Cas9 genome editing. Expected WT amplification band: 2036 bp; expected *CLN6*$^{-/-}$ amplification band: 1155 bp. **(C)** qRT-PCR using RNA extracted from *CLN6*$^{-/-}$ clone #2 shows lack of expression of *CLN6* upon removal of exon 2 and flanking regions for a total of 881 bp. Data are means ± SEM ($n = 3$); **(D)** Immunoblot analysis of WT and *CLN6*$^{-/-}$ cells showing decreased signal for endogenous CTSD and PPT1 in *CLN6*$^{-/-}$ cells, which was rescued by re-expression of myc-CLN6. Data are means ± SEM; $n = 5$ (CTSD), $n = 3$ (PPT1). Statistical differences between groups were calculated using Student's *t* test (**C** and **D**); $^{**}P < 0.01$, $^{***}P < 0.001$, NS, not statistically significant.

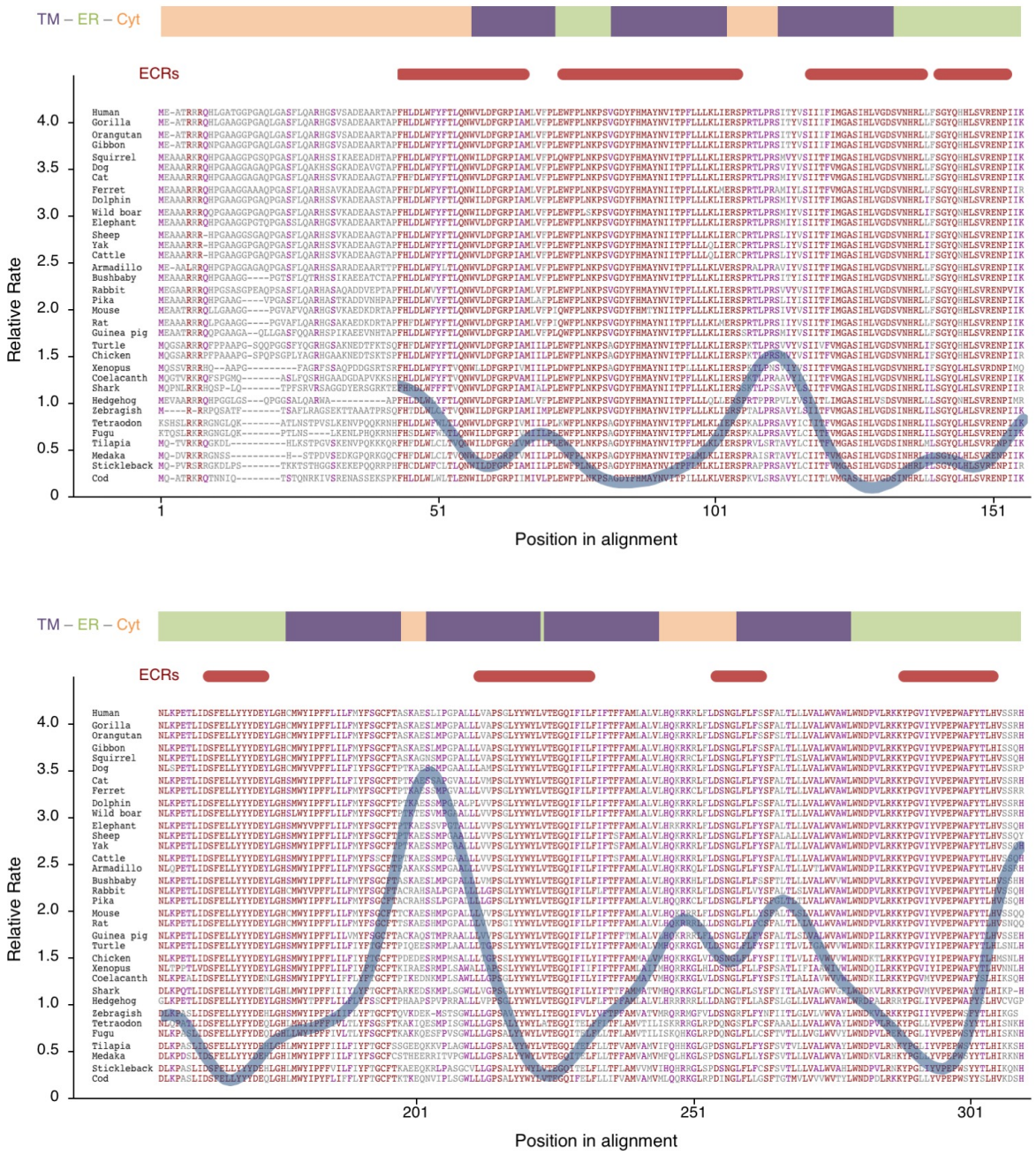

Supplemental Figure 5. Evolutionarily constrained region analysis of CLN6. Shown is a multi-alignment of CLN6 protein sequences along with a plot of local evolutionary rates. The red plot reports the average number of amino acid substitutions per site, taking into account the evolutionary relationships among proteins. Indicated are the protein transmembrane domains (TM, purple lines), cytosolic domains (Cyt, orange lines) and luminal domains (ER, green lines). Evolutionarily constrained regions (ECRs) are indicated with red lines.

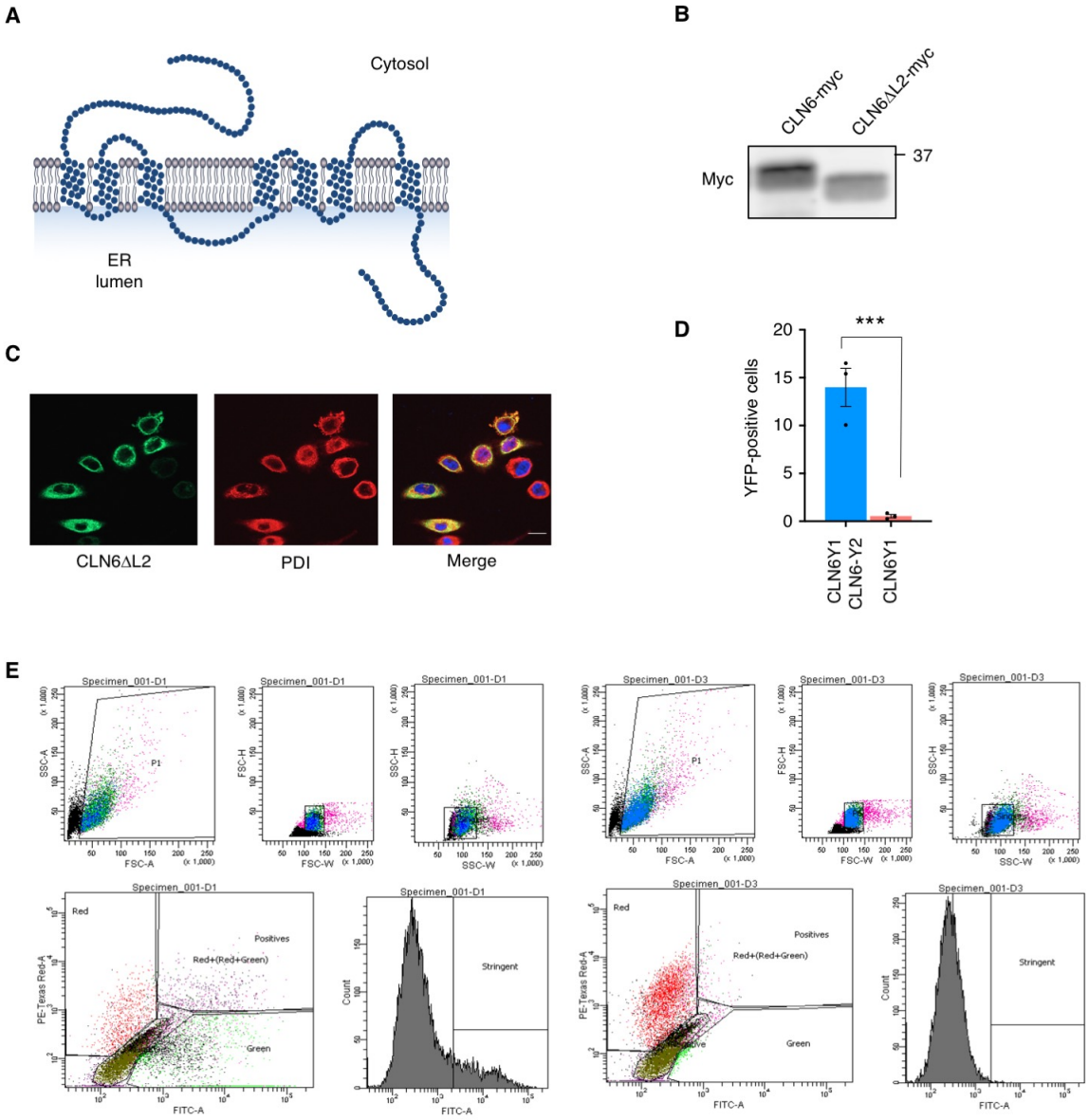

Supplemental Figure 6. Generation and expression of the CLN6ΔL2 construct and tests for CLN6 dimerization. (A) Cartoon structure of CLN6ΔL2. **(B)** Protein expression of full-length CLN6 and CLN6ΔL2, both tagged with myc. **(C)** Confocal microscopy analysis showing co-localization of CLN6ΔL2 (green) with the ER marker PDI (red). Scale bar: 20 μm. **(D)** Quantification of BiFC of CLN6-Y1 with CLN6-Y2 in HEK-293T cells by flow cytometry. CLN6-Y1 is used as a negative control. Data are means ± SEM (n = 3). **(E)** Representative gating for BiFC-flow cytometry analysis. Cells were co-transfected with split-YFP vectors and a Ruby plasmid (red fluorescence) that was used to normalize BiFC readings for transfection efficiency. CLN6 proteins form homodimers and we used this property to set up the gates for BiFC-flow cytometry assay. Shown are examples of histograms of BiFC data for CLN6-Y1/CLN6-Y2 *(left)* and CLN6-Y1 (control, *right*). Statistical differences between groups were calculated using Student's t test; ***$P < 0.001$.

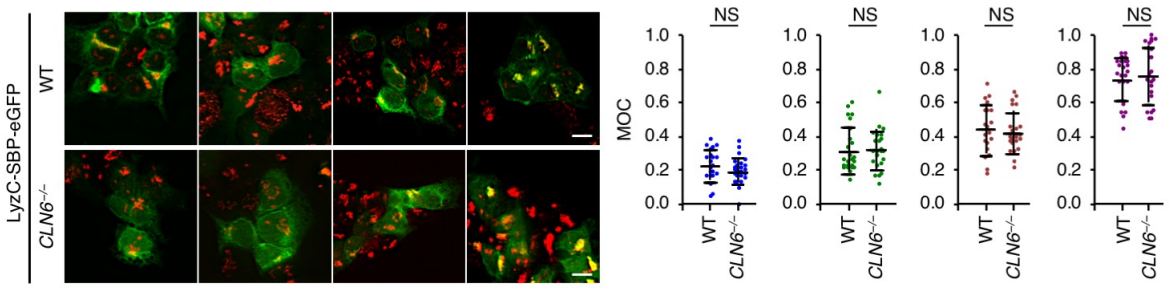

Supplemental Figure 7. CLN6 deficiency does not impair trafficking of LyzC. Confocal microscopy analysis of WT and *CLN6*$^{-/-}$ HEK293-T cells transfected with a plasmid expressing lysozyme C, a secretory protein that does not reside in the lysosome, fused with streptavidin binding protein (SBP)-eGFP (LyzC-SBP-eGFP) and streptavidin-KDEL ‘‘anchor’’ that retains SBP-containing proteins in the ER. Shown are representative images of cells without addition of biotin (0 min) and at 5, 10, and 20 min from the addition of biotin. Manders’ overlap coefficients (MOC) measuring the degree of colocalization between LyzC-SBP-eGFP (green signal) and the Golgi marker GM130 (red signal) are reported. Scale bars: 100 µm. Data are means ± SEM; WT cells, $n = 21$ (0 mins), $n = 24$ (5 mins), $n = 20$ (10 mins), $n = 23$ (20 mins); *CLN6*$^{-/-}$ cells, $n = 25$ (0 mins), $n = 23$ (5 mins), $n = 22$ (10 mins), $n = 22$ (20 mins). Statistical differences between groups were calculated using Student’s *t* test; NS, not statistically significant.

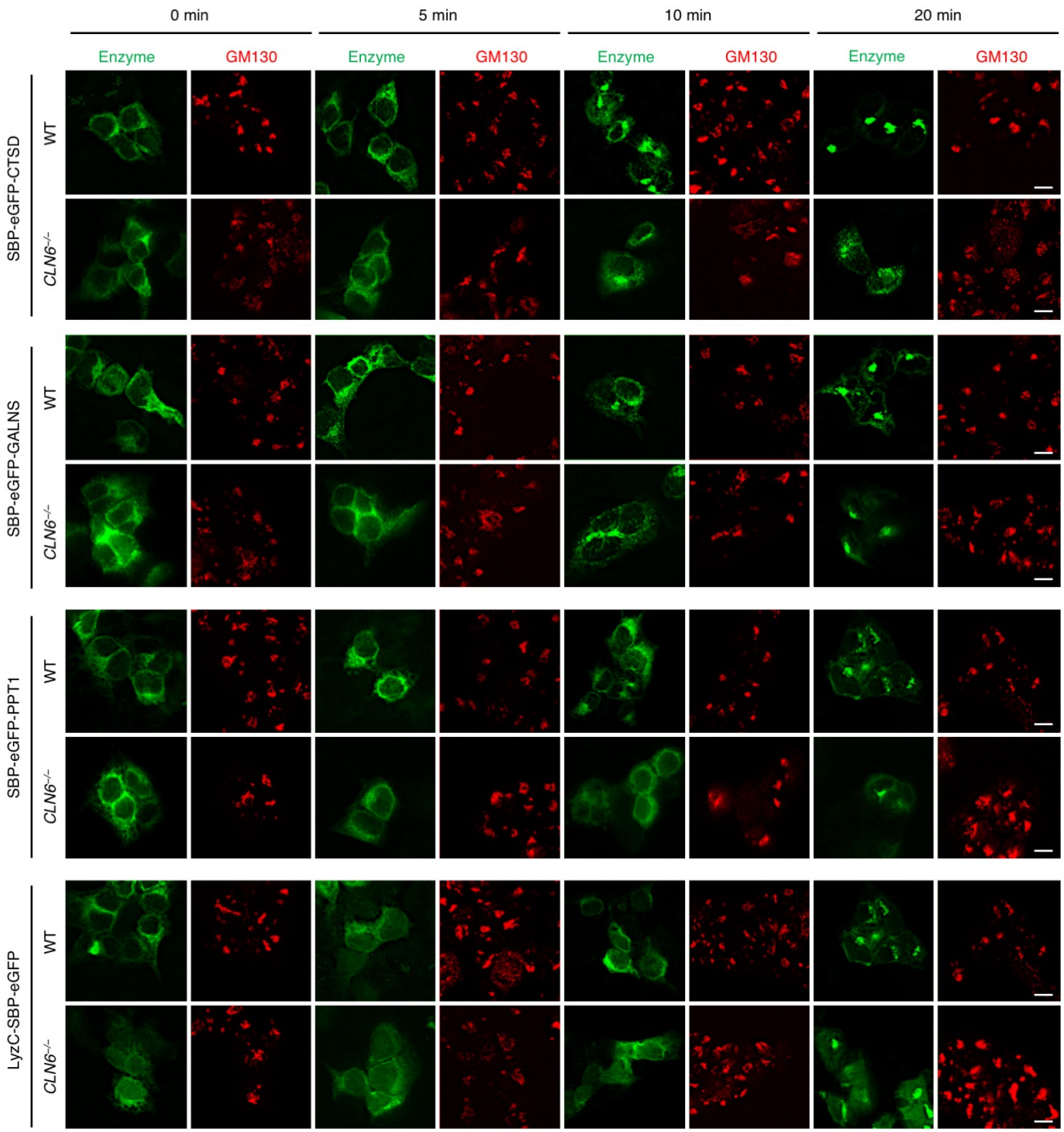

Supplemental Figure 8. Split channels of the RUSH cargo assay analysis. Single confocal microscopy channels for the analyses reported in Figure 7 and Supplemental Figure 7. Green, SBP-eGFP-fused enzyme (CTSD, GALNS, PPT1, or LYZ/LyzC). Red, Golgi protein GM130. Scale bars: 100 µm.

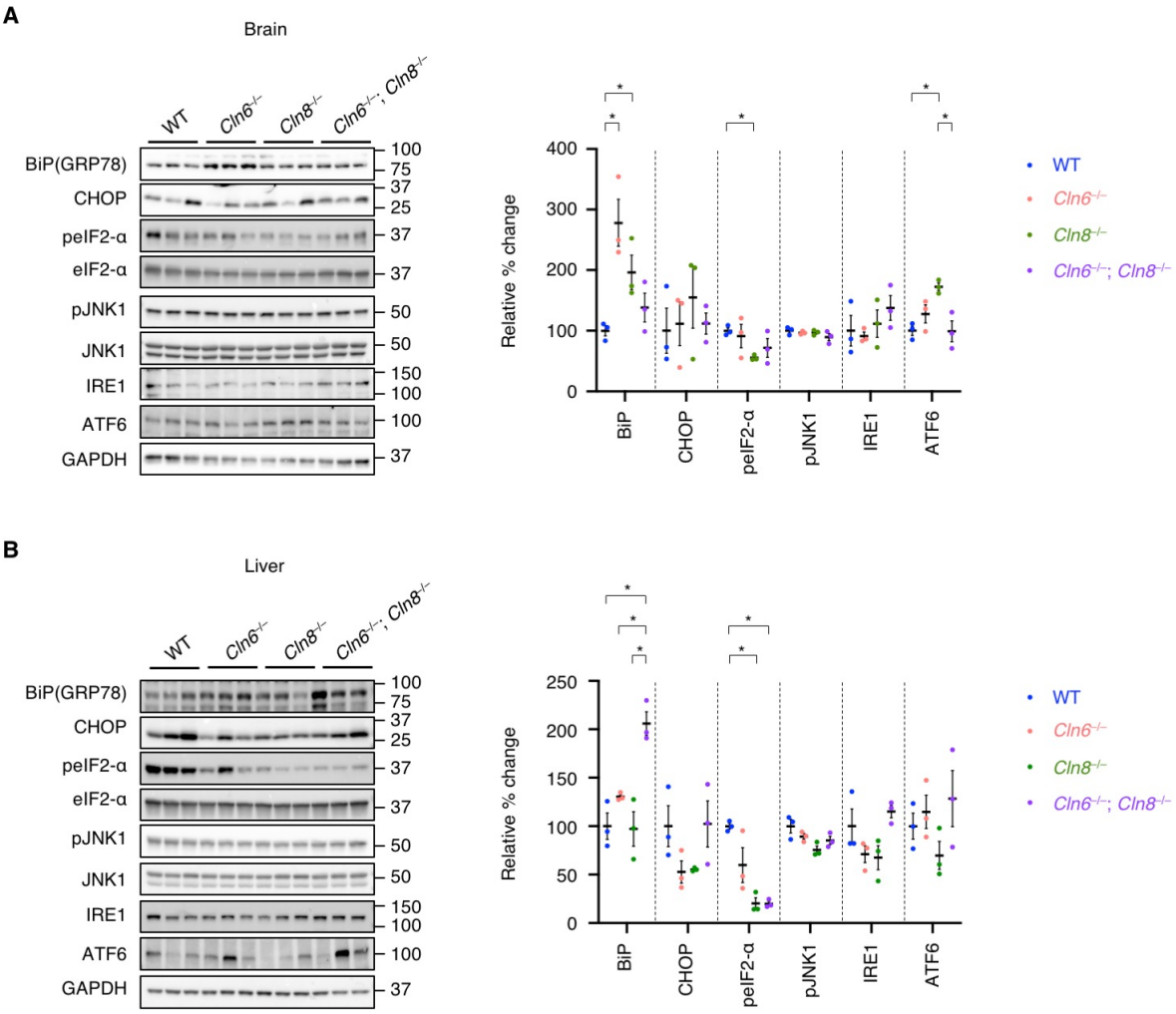

Supplemental Figure 9. Analysis of ER-stress pathways in vivo. (A) Immunoblot analysis of whole-brain homogenate from wild-type, *Cln6*$^{-/-}$, *Cln8*$^{-/-}$, and *Cln6*$^{-/-}$;*Cln8*$^{-/-}$ mice. Blots were run in parallel and band intensities were quantified and normalized to GAPDH. Data are means ± SEM ($n = 3$, *P < 0.05), paired *t* test coupled with false discovery rate (FDR) < 0.1 for multiple testing. **(B)** Immunoblot analysis of liver homogenate from wild-type, *Cln6*$^{-/-}$, *Cln8*$^{-/-}$, and *Cln6*$^{-/-}$; *Cln8*$^{-/-}$ mice. Blots were run in parallel and band intensities were quantified and normalized to GAPDH. Data are means ± SEM ($n = 3$). Statistical differences between groups were calculated using Student's *t* test coupled with false discovery rate (FDR) < 0.1 for multiple testing. *$P < 0.05$.

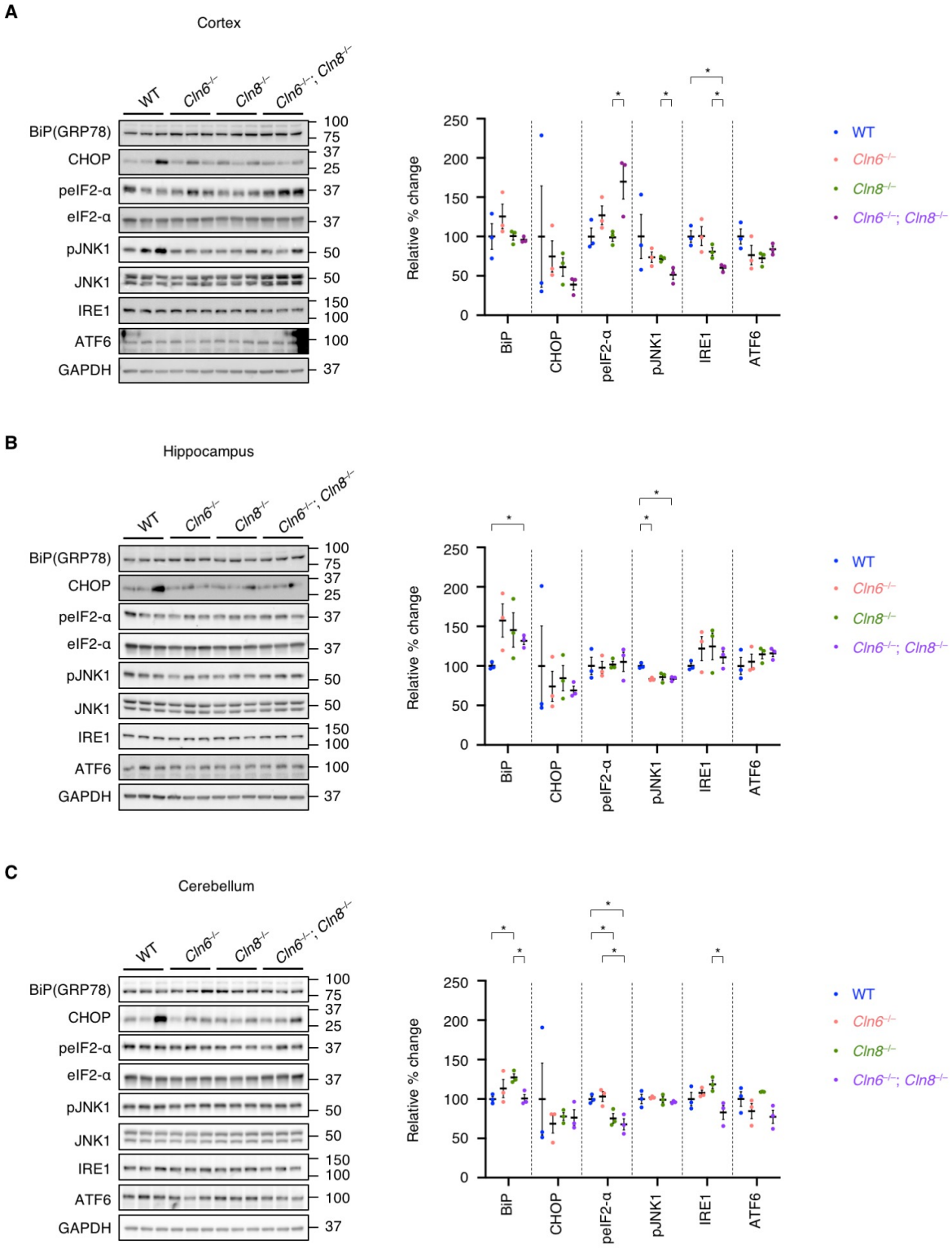

Supplemental Figure 10. Analysis of ER-stress pathways in mouse brain subregions. (A-C) Shown are immunoblot analyses of mouse brain subregions from wild-type, *Cln6*$^{-/-}$, *Cln8*$^{-/-}$, and *Cln6*$^{-/-}$; *Cln8*$^{-/-}$ mice. Blots were run in parallel and band intensities were quantified and normalized to GAPDH. Data are means ± SEM (n = 3). Statistical differences between groups were calculated using Student's *t* test coupled with false discovery rate (FDR) < 0.1 for multiple testing. **P* < 0.05.

Supplemental Table 1. FDR values of the ERG analysis.

Flash Intensity	WT, *Cln6*$^{-/-}$	WT, *Cln8*$^{-/-}$	WT, DKO	*Cln6*$^{-/-}$,*Cln8*$^{-/-}$	*Cln6*$^{-/-}$, DKO	*Cln8*$^{-/-}$, DKO
			a-wave (Scotopic)			
0.1	0.831	0.302	0.380	0.233	0.134	0.814
1	0.120	0.080	0.073	0.051	0.028	0.814
2.5	0.009	0.028	0.014	0.732	0.028	0.631
25	0.026	0.028	0.014	0.257	0.053	0.274
			b-wave (Scotopic)			
2.5	0.022	0.344	0.027	0.210	0.579	0.294
25	0.022	0.054	0.021	0.424	0.488	0.964
791	0.002	0.114	0.001	0.949	0.004	0.294
			b-wave (Photopic)			
0.001	0.210	0.089	0.242	0.307	0.905	0.445
0.01	0.074	0.052	0.026	0.623	0.412	0.820
0.1	0.101	0.052	0.041	0.521	0.035	0.820
1	0.210	0.089	0.071	0.521	0.019	0.445
2.5	0.071	0.052	0.022	0.521	0.035	0.820

Supplemental Table 2. List of antibodies.

Antibodies	Supplier	Catalog #	Host	Working dilution
	Primary antibodies			
anti-C-myc	Sigma-Aldrich	C3956-2MG	Rabbit	1:1000
anti-CTSB (CA10)	Millipore	IM27L-100UG	Mouse	1:1000
anti-CTSD (R-20)	Santacruz	sc-6487	Goat	1:1000
anti-CTSD (D-7)	Santacruz	sc-377299	Mouse	1:1000
anti-CTSD (CTD-19)	Abcam	ab6313	Mouse	1:1000
anti-GALNS	Abcam	ab187516	Goat	1:1000
anti-GAPDH (6C5)	Santacruz	sc-32233	Rabbit	1:1000
anti-GFP	Abcam	ab13970	Chicken	1:1000
anti-GFP	Cell Signaling	2956S	Rabbit	1:1000
anti-GM130	Abcam	ab526449	Rabbit	1:200
anti-KDEL (10C3)	Abcam	ab12223	Mouse	1:200
anti-LAMP1 (1D4B)	Santacruz	sc-19992	Rat	1:250
anti-LAMP2 (H4B4)	Santacruz	sc-18822	Mouse	1:1000
anti-PPT1	Santacruz	sc-130726	Rabbit	1:500
anti-PPT1	Sigma	HPA021546-100UL	Rabbit	1:1000
anti-TPP1	Santacruz	sc-393961	Mouse	1:1000
anti-TPP1 (H-300)	Santacruz	sc-66836	Rabbit	1:500
anti-NAGLU	Abcam	ab72178	Rabbit	1:500
anti-BiP (C50B12)	Cell Signaling	3177S	Rabbit	1:1000
anti-CHOP/GADD153 (B-3)	Santacruz	sc-7351	Mouse	1:500
anti-phospho-eIF2α (Ser51) (D9G8)	Cell Signaling	3398S	Rabbit	1:500
anti-eIF2α (D7D3)	Cell Signaling	5324S	Rabbit	1:1000
anti-IRE1α (14C10)	Cell Signaling	3294S	Rabbit	1:500
anti-ATF6 (D4Z8V)	Cell Signaling	65880S	Rabbit	1:500
anti-phospho-SAPK/JNK (G9)	Cell Signaling	9255S	Mouse	1:500
anti-SAPK/JNK	Cell Signaling	9252S	Rabbit	1:1000
	Secondary antibodies			
Alexa Fluor® 488 Anti-Rat IgG	Invitrogen	A-11006	Goat	1:1000
Alexa Fluor® 488 Anti-Chicken IgG	Invitrogen	A-11039	Goat	1:1000
Alexa Fluor® 488 Anti-Mouse IgG	Invitrogen	A-21200	Chicken	1:1000
Alexa Fluor® 594 Anti-Mouse IgG	Invitrogen	A-21201	Chicken	1:1000
Alexa Fluor® 594 Anti-Rabbit IgG	Invitrogen	A-21202	Donkey	1:1000
Alexa Fluor® 633 Anti-Mouse IgG	Invitrogen	A-21052	Goat	1:1000
Alexa Fluor® 633 Anti-Goat IgG	Invitrogen	A-21082	Donkey	1:1000
ECL anti-rabbit IgG-HRP	GE Healthcare	NA9340-1ML	Donkey	1:5000
ECL anti-chicken IgY-HRP	Santacruz	sc-2428	Goat	1:5000
ECL anti-goat IgG-HRP	Santacruz	sc-2020	Donkey	1:5000
ECL anti-rat IgG-HRP	GE Healthcare	NA9350-1ML	Goat	1:5000
ECL anti-mouse IgG-HRP	GE Healthcare	NA9310-1ML	Sheep	1:5000

Supplemental Table 3. Oligonucleotides used for cloning, gene/genome editing, and qRT-PC.

Name	Forward Primer	Reverse Primer
	Cloning and mutagenesis	
pIRESneo3-SS-SBP-eGFP-PPT1	agctgtacaagggccgggacccgccggcgccgc	tgatcagttatctagttatccaaggaatggtatgatgtgg
pIRESneo3-SS-SBP-eGFP-GALNS	agctgtacaagggccgggccccgcagccccccaacat	tgatcagttatctagttagtgggaccagaggcacttctt
CLN6 infusion short	cagtgtggtggaattcatggaggcgacgcggagg	ccaccgccaccatcgatgtgccgactgctgacgtgaagg
CLN8ΔL	ctggtcagcagcctgtatc	agcttggagattgaccaaag
CLN8dK	ggccctctagactcgagctatggccttcgtcgacgcagcag ctgcccgttgccttc	gaaggcaacgggcagctgctgcgtcgacgaaggccatagctcgagt ctagagggcc
	Genome editing	
CRISPR_CLN6_1	caccggtccatcaggattggtcta	caccgctctatgacttggcccgtc
CRISPR_CLN6_2	aaactagaccaatcctgatggacc	aaacgacgggccaagtcatagagc
CRISPR_CLN8_B	caccgtgtagggcccggcccgtgt	aaacacacgggccgggccctacac
CRISPR_CLN8_D	caccgcgccctttacctgcgtttcc	aaacggaaacgcaggtaaagggcgc
DNA_check_CLN6	ttgggaaaagcttcatcagg	ggtgctccacttcctttcct
qRT_CRISPR CLN6	aggccaggcatggctct	ggaataccagcatggcaatg
CLN8_entryclone	ttgctcgagggaattcatgaatcctgcgagcgatggg	cgcaccgggcgaattccttacatattcagatcctcttctga
CLN8_KI_check	agcataggaccgtgtgttcc	aaaggtagccaggtgtggtg
	RT-qPCR	
Cyclophilin	ggcaaatgctggaccaaacacaa	gtaaaatgcccgcaagtcaaaag
Ctsb	ttgcgttcggtgaggacatag	aaatgcccaacaagagccg
Ctsd	cgtcctttgacatccactacgg	tggaaccgatacagtgtcctgg
Gaa	ctcctacccaggtcc	atggccaggctcttgttgtcag
Glb1	aaatggctggcagtccttctg	acctgcacggttatgatcggt
Tpp1	cccctcatgtggattttgtgg	tggttctggacgttgtcttgg